Trend in Fine Sulfate Concentrations and the Associated Secondary Formation Processes at an Urban Site in North China

Yating Zhang[1], Liang Wen[1], Jianmin Chen[1,2], Xinfeng Wang[1*], Likun Xue[1], Lingxiao Yang[1], Liwei Wang[1], Zeyuan Li[1], Chuan Yu[1], Tianshu Chen[1], Wenxing Wang[1]

[1] *Environment Research Institute, Shandong University, Ji'nan 250100, China*
[2] *Shanghai Key Laboratory of Atmospheric Particle Pollution and Prevention, Department of Environmental Science and Engineering, Institute of Atmospheric Sciences, Fudan University, Shanghai 200433, China*

ABSTRACT

There has been a significant decline in SO_2, the main precursor of sulfate, in North China over the past decade due to strict sulfur removal measures, whereas the amount of photochemical oxidants such as ozone has continued to increase in this region. In this study, we examined temporal variation in the concentrations of fine sulfate in urban Ji'nan in North China from 2008 till 2015. Over this period, the sulfate concentration decreased by -3.86 ± 2.50 µg m^{-3} yr^{-1} (-10.0 % yr^{-1}), which is slower that the rate of decrease for SO_2 during the same period (-11.6 % yr^{-1}). Nevertheless, the sulfur oxidation ratio and the concentrations of ozone and calcium (an indicator of dust particles) increased over this period. An analysis of the seasonal and diurnal variations in sulfate and the related parameters in 2015 indicated that the ambient sulfate concentration was largely influenced by the amount of SO_2, atmospheric oxidants, aerosol loading, and meteorological conditions. A detailed investigation of the production of sulfate in eight case studies found that the observed sulfate production rate was in the range of 1.1–10.8 µg m^{-3} h^{-1}. Numerical calculations revealed that SO_2 oxidation by OH and H_2O_2 was a major contributor to sulfate production during the daytime in warm seasons. At all times of the day in cold seasons and at nighttime in warm seasons, the heterogeneous SO_2 reaction on aerosol surfaces contributed 30.1%–65.7% of the sulfate production. The increasing amount of ozone and dust particles in this region, which are associated with photochemical pollution and urban dust emissions, are responsible for the slower decrease in sulfate concentration. Therefore, photochemical smog and urban dust should receive adequate attention in order to mitigate the sulfate pollution.

Keywords: Fine sulfate; Decreasing trend; Formation pathways; Photochemical oxidants; Dust particles.

INTRODUCTION

Fine particulate matter pollution has frequently occurred in China in the past decade owing to the rapid urbanization and the concentrated industries (Yue *et al*., 2015; Fang *et al*., 2017; Li *et al*., 2017b; Li *et al*., 2018). Sulfate (SO_4^{2-}) is an important secondary inorganic component in fine particulate matters and has an adverse impact on air quality, climate change, ecosystems, and human health (Seinfeld and Pandis, 2006; Fang *et al*., 2016). Sulfate contributes a large fraction to $PM_{2.5}$, ranging from 10% to 35% in urban areas in China (Cao *et al*., 2012; Yang *et al*., 2012; Huang *et al*., 2014a; Huang *et al*., 2017; Fang *et al*., 2017). High loadings of sulfate aerosols are significant contributors to haze formation and have led to frequent haze episodes in

North China (Zhao *et al*., 2013; Wang *et al*., 2014ba; Jiang *et al*., 2015). In addition, sulfate aerosols are hygroscopic and act as efficient cloud condensation nuclei, which affect cloud formation and precipitation (Li *et al*., 2008; Wang *et al*., 2011). Furthermore, they exert an important cooling effect on the climate (Li *et al*., 2016). The deposition of sulfates causes soil and lake acidification, which is a serious threat to the earth's ecosystem (Zhao *et al*., 2009). Sulfate aerosols also directly endanger human health by invading respiratory systems (Pope III *et al*., 2002).

Sulfate can be produced by multiple formation pathways and the contributions of the different pathways vary with the concentrations of precursors, oxidants, aerosol properties, dust particles, and meteorological conditions. The gas-phase oxidation of SO_2 by OH radicals produces sulfuric acid during the daytime, which in turn promotes new particle formation. The aqueous oxidation of SO_2 involves H_2O_2, O_3, NO_2, and O_2 (catalyzed by transition metals) and occurs within both small cloud/fog droplets and in the surface liquid water layer of aerosols (Seinfeld and Pandis, 2006). The aqueous formation pathways of sulfate largely depend

---

on aerosol acidity, due to its influence on the solubility of SO_2 and the subsequent ionic forms. At a low aerosol pH (< 4.5), H_2O_2 oxidation is generally the fastest pathway for aqueous sulfate formation (Shen *et al.*, 2012). However, at a high aerosol pH (> 5.5), O_3 and NO_2 act as the most important oxidants (Shen *et al.*, 2012; Cheng *et al.*, 2016; Wang *et al.*, 2016a; Xue *et al.*, 2016a). The heterogeneous reaction of SO_2 on the surfaces of aerosols (in particular dust particles) also produces sulfate, with a production rate that is largely influenced by aerosol surface area density and humidity (Fairlie *et al.*, 2010; Wang *et al.*, 2012; He *et al.*, 2014; Liu *et al.*, 2015b; Fu *et al.*, 2016). To date, other formation pathways of sulfate, including gas-phase oxidation of SO_2 by Criegee intermediates and aqueous oxidation involving organic peroxides and OH radicals, have not been well configured. Because of the large diversity in global atmospheric constitutions, the predominant formation pathways and the key influencing factors vary between locations and must be evaluated locally.

To mitigate sulfate aerosol pollution and its environmental impacts, a series of strict sulfur removal measures have been implemented in China over the past decade. There has been a significant decline in the SO_2 column concentration in the North China Plain since 2008 (Krotkov *et al.*, 2016). Nevertheless, over the past decade, photochemical pollution has increased and the atmospheric oxidation capability in North China has also increased, as indicated by the rising amount of ozone (Ma *et al.*, 2016; Sun *et al.*, 2016). In addition, dust pollution remains serious in some urban areas in North China, mainly due to the rapid urbanization in recent years (Anonymity, 2017). Therefore, it is essential to assess the temporal trends in sulfate concentrations and how its formation processes respond to changing precursors, oxidants, and dust particles in this region.

Ji'nan, the capital city of Shandong Province, is located almost in the center of North China. Due to the intensive emissions of air pollutants from various anthropogenic sources, urban Ji'nan has suffered from serious particulate matter and photochemical pollution in the past decade and sulfate is one of the major contributors to haze episodes (Gao *et al.*, 2011; Wang *et al.*, 2014b). In this study, we examined the temporal trends in fine sulfate and the sulfate oxidation ratio in urban Ji'nan over the 2008 to 2015 period. To understand the formation processes of sulfate associated with the variation trend in the region, seasonal and diurnal variations of sulfate and the key influencing factors in 2015 were analyzed and the production rates of sulfate via various formation pathways were explored in detail.

DATA AND METHODOLOGY

Field Measurements
Sampling Site and Period
The field measurements were conducted at the Atmosphere Environment Observation Station located on top of a seven-story teaching building on the Central Campus of Shandong University (SDU-CC; 36°40′N, 117°03′E, ~22 m above ground level), in urban Ji'nan (see Fig. 1). The sampling site was surrounded by residential, educational and commercial districts and there were several major and minor roads nearby. In the past decade, Ji'nan has experienced intensive urban development and the area of land for construction increased 64.8% between 2005 and 2015 (Shandong Provincial Bureau of Statistics, http://www.stats-sd.gov.cn/col/col211/index.html). Field measurements of water-soluble ions, trace gases, $PM_{2.5}$ concentrations, and meteorological parameters were carried out from March 26 to November 30, 2015.

Measurement Instruments
The major water-soluble inorganic ions in $PM_{2.5}$ were measured using the monitor for aerosols and gases in ambient air (MARGA, ADI 2080, Applikon-ECN, Netherlands). Briefly, the sampling system was composed of two parts: a wet rotating denuder that captured the acidic and alkaline gases (HCl, NH_3, HNO_2, and HNO_3) and a steam jet
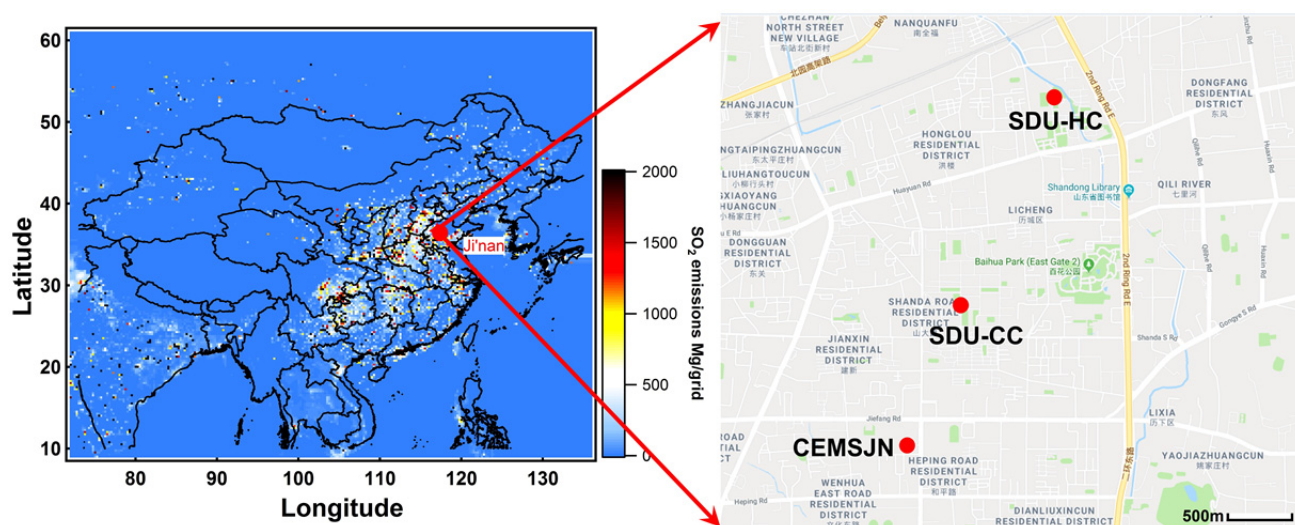

Fig. 1. Maps showing the locations of the sampling sites in urban Ji'nan in North China. The left map is color-coded to show SO_2 emission intensity in 2010 retrieved from MIX emission inventory (Li *et al.*, 2017a).

aerosol collector that collected the inorganic ions (SO_4^{2-}, NH_4^+, NO_3^-, NO_2^-, Mg^{2+}, Ca^{2+}, K^+, Cl^-, and Na^+). The sample solutions were analyzed hourly by two ion chromatographs with eluents of $NaHCO_3$-Na_2CO_3 for anions and methanesulfonic acid for cations. The contents of the water-soluble ions and the acidic and alkaline gases were quantified using multi-point standard curves and the LiBr internal standard. This technique has been applied in several field campaigns and was described in detail in our previous study (Wang *et al.*, 2015).

PM$_{2.5}$ concentrations were measured using a particle monitor (SHARP, Model 5030, Thermo Scientific, USA) based on the scattering coefficient of 880 nm light and the absorption coefficient of beta rays. The surface area density of the aerosols in the range 5 nm to 1 μm was quantified using a wide-range particle spectrometer (WPS, Model 1000XP, MSP Corporation, USA). Concurrently, some other trace gases were monitored with online analyzers. SO$_2$ was measured with a UV fluorescence analyzer (Model 43C, Thermo Environment Instruments (TEI), USA). Ozone was detected using a commercial ultraviolet photometric technique (Model 49C, TEI). NO$_2$ was monitored by a chemiluminescence analyzer equipped with an internal MoO catalytic converter (Model 42C, TEI). In addition, meteorological parameters including relative humidity, ambient temperature, wind speed, and wind direction were monitored by an automatic meteorological station (Huayun, China).

Historical Data Collection

To evaluate trends in the inter-annual variations of fine sulfate concentrations and the influencing factors in urban Ji'nan, we collected available historical data on sulfate concentrations and related air pollutants in urban Ji'nan (see Table 1). The data of sulfate and calcium in PM$_{2.5}$ for the periods between December 2007 and October 2008 were obtained from an online ambient ion monitor (AIM, 9000B, URG, USA) with a time resolution of 1 h (Gao *et al.*, 2011). In 2010, ion chromatography in a laboratory was used to measure the daily concentrations of sulfate and calcium in PM$_{2.5}$ filter samples (Gu *et al.*, 2014). The PM$_{2.5}$ data for 2008 and 2010 were determined by filter sampling and weighing with a time resolution of 12–24 h. The methods and instruments used in 2013 were the same as those used in 2015. Trace gases of SO$_2$ and O$_3$ for all of the periods were measured with online gas analyzers, Model 43C and Model 49C, respectively.

Three sampling sites have been used in previous field measurements in urban Ji'nan (also shown in Fig. 1). The first site was located in the Central Campus of Shandong University (Gao *et al.*, 2011), and is the same site used for the 2015 measurements. The second site was in the Hongjialou Campus of Shandong University (SDU-HC, 36°41′N, 117°04′E), which is 1.8 km northeast of the SDU-CC site (Xu *et al.*, 2011). The third site was in the Central Environment Monitoring Station of Ji'nan (CEMSJN, 36°40′N, 117°03′E), which is 1.1 km south of the SDU-CC site (Gu *et al.*, 2014). All of the three sampling sites are located in urban areas and are surrounded by educational,

residential, and commercial districts with no large-scale emission source nearby. Therefore, the change of the sampling sites is believed having little influence on the long-term trends.

Calculation of Sulfate Production Rate

To identify the dominant factors in fine sulfate formation in pollution episodes in urban Ji'nan, the production rates of the five formation pathways of sulfate (P), including gas-phase SO$_2$ oxidation by OH radicals, aqueous oxidation of SO$_2$ with H$_2$O$_2$, O$_3$, and NO$_2$, and the heterogeneous process of SO$_2$, were calculated according to the methods described in previous studies (see Table 2). The calculation formulas are expressed as follows:

$$P(OH) = k_1[OH][SO_2] \tag{1}$$

$$P(H_2O_2) = k_2[H_2O_{2(aq)}][H^+][HSO_3^-] \tag{2}$$

$$P(O_3) = k_3[SO_2 \cdot H_2O + HSO_3^- + SO_3^{2-}][O_{3(aq)}] \tag{3}$$

$$P(NO_2) = k_4[HSO_3^-][NO_{2(aq)}] \tag{4}$$

$$P(aerosol) = 1/4\gamma_{SO2}\upsilon_{SO2}S_P[SO_2] \tag{5}$$

here, [OH] and [SO$_2$] represent the abundances of OH radicals and SO$_2$, respectively. [SO$_2$·H$_2$O], [HSO$_3^-$], [SO$_3^{2-}$], and [H$^+$] represent the respective concentrations in the aqueous phase. [H$_2$O$_{2(aq)}$], [O$_{3(aq)}$], and [NO$_{2(aq)}$] represent the concentrations of H$_2$O$_2$, O$_3$, and NO$_2$ dissolved in the aqueous phase, respectively. k$_1$ is the gas-phase reaction rate constant of SO$_2$ with the OH radical. k$_2$, k$_3$, and k$_4$ represent the reaction rate constants of dissolved SO$_2$ with H$_2$O$_2$, O$_3$, and NO$_2$ in the aqueous phase, respectively. The γ_{SO2} is the uptake coefficient of SO$_2$ on the aerosol surface and ranges from 0.7×10^{-5} to 1.8×10^{-5}. υ_{SO2} expresses the average molecular velocity of SO$_2$, and S$_P$ indicates the aerosol surface area density.

The aqueous water content, aqueous-phase concentration of H$^+$, and aerosol pH were calculated with the online ISORROPIA-II thermodynamic model (Fountoukis and Nenes, 2007; Liu *et al.*, 2017). The concentrations of H$_2$O$_2$, O$_3$, and NO$_2$ in the aqueous phase were assumed to be in equilibrium with their gas-phase concentrations and were calculated based on the following formulas:

$$[O_x(aq)] = P(O_x)H(O_x) \tag{6}$$

$$[SO_2 \cdot H_2O] = P(SO_2)H(SO_2) \tag{7}$$

here, [O$_x$(aq)] represents the concentrations of oxidants O$_x$ (H$_2$O$_2$, O$_3$, and NO$_2$). [SO$_2$·H$_2$O] represents the concentrations of dissolved SO$_2$ in the aqueous phase. P(O$_x$) and P(SO$_2$) are the partial pressures of O$_x$ and SO$_2$, respectively. H(O$_x$) and H(SO$_2$) are the Henry's law constants of O$_x$ and SO$_2$, respectively. The dissociated components of HSO$_3^-$ and SO$_3^{2-}$ can be expressed by Eqs. (8) and (9), respectively:

$$[HSO_3^-] = k_{S1}P(SO_2)H(SO_2)/[H^+] \tag{8}$$

Table 1. Average concentrations of sulfate, SO_2, SOR, O_3, $PM_{2.5}$, and Ca^{2+} in four seasons at urban sites in Ji'nan in 2008, 2010, 2013, and 2015. The data are from previous studies and observations made during this study.

Year	Site	Periods	SO_4^{2-} (μgm^{-3})	SO_2 (ppb)	SOR	O_3 (ppb)	$PM_{2.5}$ (μgm^{-3})	Ca^{2+} (μgm^{-3})	Reference
2008	SDU-CC, SDU-HC	Average	38.3	37.0	0.26	25.1	140.9	0.76	Gao *et al.*, 2011; Xu *et al.*, 2011
		Winter(12/01/2007–01/03/2008)	42.8	58.6	0.17	6.8	159.6	1.41	
		Spring (04/01–04/18/2008)	27.2	32.1	0.22	38.8	102.7	0.83	
		Summer (06/05–06/17/2008)	64.3	26.3	0.47	45.9	173.2	0.29	
		Autumn (09/12–10/15/2008)	31.0	22.3	0.30	28.3	99.3	0.23	
2010	CEMSJN	Average	47.9	32.5	0.30		166.7	2.42	Gu *et al.*, 2014
		Spring (18 days)	26.0	21.5	0.22		144.5	2.93	
		Summer (11 days)	62.0	11.8	0.55		145.4	0.98	
		Autumn (17 days)	52.0	23.6	0.34		133.3	1.05	
		Winter (14 days)	60.0	73.5	0.16		252.6	4.58	
2013	SDU-CC	Average	23.3	29.6	0.20	31.1	129.5	1.98	Wang *et al.*, 2015, this study
		Spring (03/01/2013–04/29/2013)	19.8	23.7	0.21	38.2	84.4	2.21	
		Summer (07/01–08/31/2013)				49.5			
		Autumn (10/11–11/14/2013)	22.4	17.3	0.28	28.1	113.2	1.54	
		Winter (12/18/2013–02/15/2014)	27.4	42.7	0.14	12.9	145.8	2.01	
2015	SDU-CC	Average	15.6	8.2	0.36	38.1	91.7	4.36	This study
		Spring (03/27–05/31/2015)	14.2	8.1	0.39	35.8	83.9	4.81	
		Summer (06/01–07/31/2015)	17.8	4.9	0.48	50.4	47.0	5.60	
		Autumn (09/01/2015–11/14/2015)	13.7	9.6	0.26	35.2	96.0	3.53	
		Winter (11/15–11/30/2015)	19.6	14.1	0.27	12.4	132.1	2.48	

Table 2. Five formation pathways of sulfate and the calculation formulas for their production rates.

Reactions/ Solution/ Dissociation equilibrium	Reaction rate (M/s or molecule/(cm³ s))/Henry's law constant (M atm⁻¹)/Dissociation constant (M)	References
Gas-phase Reaction		
Eq. (1)[a] $OH + SO_2 + M \rightarrow sulfate + HO_2$	$P(OH) = k_1[OH][SO_2]$ $k_1 = (k_{low}[M]/(1 + k_{low}[M]/k_{high})) \times 0.6^Z$ $Z = (1+(log_{10}(k_{low}[M]/k_{high}))^2)^{-1}$ $k_{low} = 3.3E{-}31 \times (T/300)^{-4.3}$, $k_{high} = 1.6E{-}12$, $[M] = 2.7E19$	Seinfeld and Pandis, 2006; Cheng et al., 2016
Aqueous-phase Reactions		
Eq. (2) $HSO_3^- + H^+ + H_2O_2(aq) \rightarrow SO_4^{2-}$	$P(H_2O_2) = k_2[H_2O_2(aq)][H^+][HSO_3^-]$ $k_2 = (7.45E7 \times exp(-4430 \times g(T))/(1 + 13 \times [H^+])$	Seinfeld and Pandis, 2006
Eq. (3)[b] $S(IV) + O_3(aq) \rightarrow SO_4^{2-}$	$P(O_3) = (k_{31}[SO_2 \cdot H_2O] + k_{32}[HSO_3^-] + k_{33}[SO_3^{2-}])[O_3(aq)]$ $k_{31} = 2.4E4$ $k_{32} = 3.7E5 \times exp(-5530 \times g(T))$ $k_{33} = 1.5E9 \times exp(-5280 \times g(T))$	Seinfeld and Pandis, 2006
Eq. (4)[c] $HSO_3^- + NO_2(aq) \rightarrow SO_4^{2-}$	$P(NO_2) = k_4[HSO_3^-][NO_2(aq)]$ $k_4 = -7.16E4 \times pH^2 +5\ E6 \times pH$	Sarwar et al., 2013
Heterogeneous Reaction		
Eq. (5)[d] $SO_2 + aerosol\ surface \rightarrow SO_4^{2-}$	$P(aerosol) = (1/4\gamma_{SO2}\upsilon_{SO2}S_P)[SO_2]$ $\gamma_{SO2} = \gamma_{low} + (\gamma_{high}-\gamma_{low})/(1 - 0.5) \times (RH - 0.5)$ $\gamma_{low} = 1E{-}5,\ \gamma_{high} = 2E{-}5$ $\upsilon_{SO2} = SQRT(8 \times 8.314 \times T \times 1E3/(64 \times P(I)))$	Zheng et al., 2015
Solution equilibrium		
Eq. (6) $H_2O_2(g) \leftrightarrow H_2O_2(aq)$ $O_3(g) \leftrightarrow O_3(aq)$ $NO_2(g) \leftrightarrow NO_2(aq)$ Eq. (7) $SO_2(g) \leftrightarrow SO_2 \cdot H_2O(aq)$	$H_{H2O2} = 1E5 \times exp(7297.1 \times g(T))$ $H_{O3} = 1.1E{-}2 \times exp(2536.4 \times g(T))$ $H_{NO2} = 1E{-}2 \times exp(2516.2 \times g(T))$ $H_{SO2} = 1.23 \times exp(3145.3 \times g(T))$	Seinfeld and Pandis, 2006
Dissociation equilibrium		
Eq. (8) $SO_2 \cdot H2O \leftrightarrow H^+ + HSO_3^-$ Eq. (9) $HSO_3^- \leftrightarrow H^+ + SO_3^{2-}$	$k_{S1} = 1.3E{-}2 \times exp(1960 \times g(T))$ $k_{S2} = 6.6E{-}8 \times exp(1500 \times g(T))$	Seinfeld and Pandis, 2006

[a] [M]: the concentration of N_2 and O_2.
[b] $S(IV) = SO_2 \cdot H_2O+HSO_3^-+SO_3^{2-}$, $g(T) = 1/T-1/298$.
[c] pH: aerosol acidity.
[d] γ_{SO2}: uptake coefficient of SO_2, υ_{SO2}: mean molecular velocity of SO_2 (m s⁻¹), S_P: aerosol surface area density.

$$[SO_3^{2-}] = k_{S1}k_{S2} P(SO_2)H(SO_2)/[H^+]^2 \qquad (9)$$

here, k_{S1} and k_{S2} are dissociation constants of HSO_3^- and SO_3^{2-}, respectively.

RESULTS AND DISCUSSION

Temporal Trend of Fine Sulfate

Fig. 2(a) shows the trend in fine sulfate concentration in urban Ji'nan for the 2008 to 2015 period. Note that the 2013 data was excluded when deriving the trend due to a lack of summer data (same to the trends for SO_2, SOR, $PM_{2.5}$ and calcium in Fig. 2). As shown, the annual average concentration of fine sulfate decreased at a rate of -3.86 ± 2.50 µg m^{-3} yr^{-1} (equivalent to -10.0 % yr^{-1}, $p = 0.34$). The precursor SO_2 also exhibited a decreasing trend during the same period, with a declining rate of -4.26 ± 0.58 ppbv yr^{-1} (equivalent to -11.6 % yr^{-1}, $p = 0.05$) (also see Fig. 2(a)). To verify the decreasing trends of sulfate and SO_2, the seasonal average concentrations of fine sulfate and SO_2 as well as meteorological parameters of temperature, humidity, and wind speed in urban Ji'nan for the 2008 to 2015 period were also examined (shown in Fig. S1 and Table S1). The small differences of meteorological parameters among the four years indicate little influence on the variation of air pollutants. As shown, the sulfate and SO_2 exhibited decreasing trends in all four seasons, confirming the decrease of sulfate and SO_2 in urban Ji'nan in the 2008 to 2015 period.

The decreasing amounts of sulfate and SO_2 during the 2008 to 2015 period have been attributed to the reduction in SO_2 emissions over the past decade. The reduction in SO_2 emissions in China is mainly due to the installation of flue gas desulfurization (FGD) systems in power plants, the use of clean combustion technology in industry boilers, the application of a new vehicle standard in transportation, and the use of clean fuel in the residential sector (Wang *et al.*, 2014a). The total emission of SO_2 from coal-fired power plants in China was estimated to have decreased by 54% between 2006 and 2010 owing to the installation of FGD systems (Liu *et al.*, 2015a) and by a further 19% from 2011 to 2014 due to improvements in the removal efficiency of FGD systems (Xia *et al.*, 2016). The significant drop in SO_2 emissions has resulted in the reduction of ambient SO_2 concentrations. The SO_2 vertical column concentration in East China decreased by 8.5% from 2008 to 2011 and 53.2% from 2011 to 2014 (Fu *et al.*, 2017). Similarly, the ambient concentrations of SO_2 and sulfate significantly decreased in urban Ji'nan from 2008 to 2015.

Notably, the sulfate concentration decreased at a substantially slower rate (-10.0 % yr^{-1}) than the SO_2 mixing ratio (-11.6 % yr^{-1}), which is consistent with the increasing sulfur oxidation ratio (SOR, the mole ratio of sulfate to the sum of sulfate and SO_2) (Wang *et al.*, 2005) in urban Ji'nan from 2008 to 2015 (shown in Fig. 2(b) and Fig. S1(c)). Sulfate formation and the concentration are usually dependent on characteristics of the atmospheric pollution and the formation mechanisms of sulfate and are influenced by the oxidant mixing ratio, aerosol loading and properties, and meteorological conditions. With examination of the trends
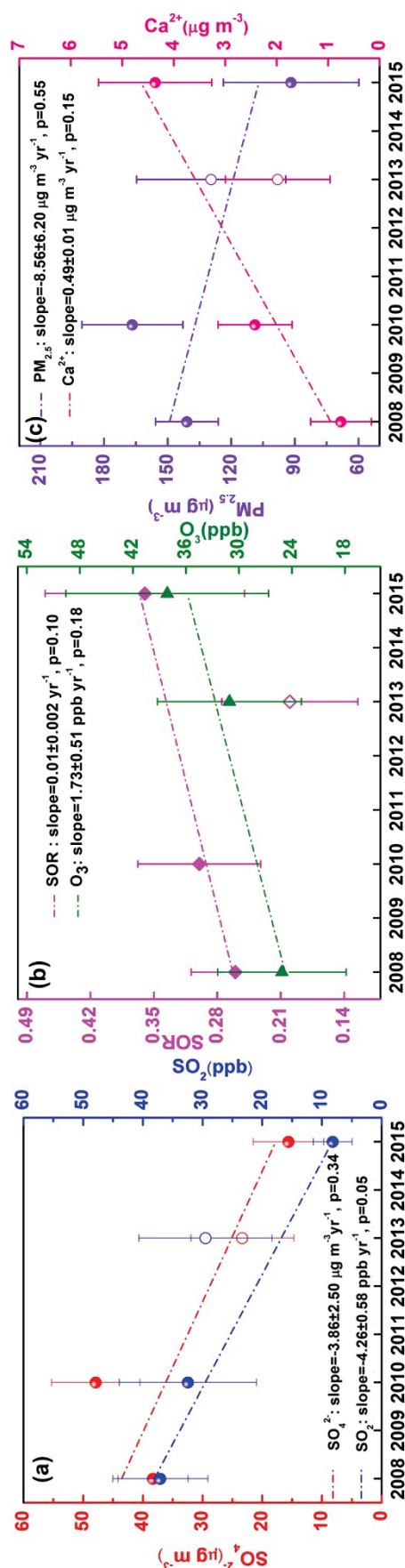

Fig. 2. Annual average values and trends in (a) fine sulfate and SO_2 concentrations, (b) SOR and O_3 mixing ratio, and (c) $PM_{2.5}$ and Ca^{2+} concentrations in the 2008 to 2015 period. The fitted lines are derived from the least square linear regression analysis and the significance levels (p) are annotated. The 2013 data of sulfate, SO_2, SOR, $PM_{2.5}$ and Ca^{2+} are marked in hollow and are excluded when driving the trend lines due to a lack of summer data.

in the concentrations of oxidants and aerosols (see Figs. 2(b) and 2(c) and Fig. S1), the enhancements of atmospheric oxidants (indicated by O_3) and the increase in dust particles (indicated by calcium) in urban Ji'nan were possibly the major factors that facilitated the SOR and thus led to the slowness of the sulfate concentration reduction. The impacts of the various influencing factors on the concentration and formation of fine sulfate in urban Ji'nan were analyzed in detail in this study and the results are presented in the following sections.

Seasonal and Diurnal Variations of Sulfate

To understand the pollution characteristics of concentrations of fine sulfate and the associated factors, the seasonal variations in the concentrations of fine sulfate, SO_2, O_3, and $PM_{2.5}$ in urban Ji'nan in 2015 are depicted in Fig. 3 and the diurnal variations of these pollutants and the meteorological parameters are illustrated in Fig. 4.

As shown in Fig. 3, there were elevated concentrations of fine sulfate in summer and winter and relatively low levels in spring and autumn, these variations were associated with the mixing ratios of precursor SO_2 and oxidants and with the aerosol loading. The average concentration of fine sulfate was highest in July, 19.6 µg m^{-3} (as shown in Fig. 3), which was linked to high levels of photochemical oxidants (e.g., 57.0 ppbv of ozone, much higher than in other months due to intensive solar radiation). In November, the average sulfate concentration reached 18.2 µg m^{-3}, which was accompanied by the highest concentrations of SO_2 (12.5 ppbv) and $PM_{2.5}$ (126.8 µg m^{-3}). Therefore, high levels of SO_2, oxidants, and aerosols together led to elevated concentrations of fine sulfate in summer and winter in urban Ji'nan.

As shown in Fig. 4, in urban Ji'nan there was a broad peak in fine sulfate concentration during the daytime (10:00–16:00 in spring, summer, and autumn and 9:00–13:00 in winter), with the maximum average hourly concentration of 15.5–21.9 µg m^{-3} appearing between 11:00 and 14:00 in all four seasons. The precursor SO_2 had a daytime concentration peak similar to that of sulfate, however, the concentration peak of sulfate emerged after a time lag of 1–3 h. Ozone, one of the representative photochemical oxidants, also exhibited a broad peak lasting from morning to early evening, with a maximum average hourly concentration of 19.3–82.7 ppbv. The above results indicate the strong dependence of sulfate concentration on the levels of precursors and oxidants. Sulfate concentrations occasionally peaked late at night, possibly due to elevated levels of SO_2 and aerosols and high humidity.

Sulfate Formation and the Contributions of Different Pathways

To further understand the dominant formation pathways of fine sulfate in urban Ji'nan and the dominant factors influencing the formation processes, eight pollution cases that had persistent increases in sulfate concentrations that lasted longer than two hours were analyzed in detail (see Fig. 5; there are four daytime cases (May 15, September 11, November 12, and November 15) and four nighttime cases (April 28, May 6, September 9, and November 11)). The selected cases had a stable wind direction, a low wind speed (mostly below 2 m s^{-1}), relatively high sulfate concentrations (maximum hourly concentration generally above 20 µg m^{-3}), and low levels of SO_2 (maximum hourly concentration mostly below 30 ppbv), indicating there was little effect from the freshly emitted SO_2 plume and the change of air
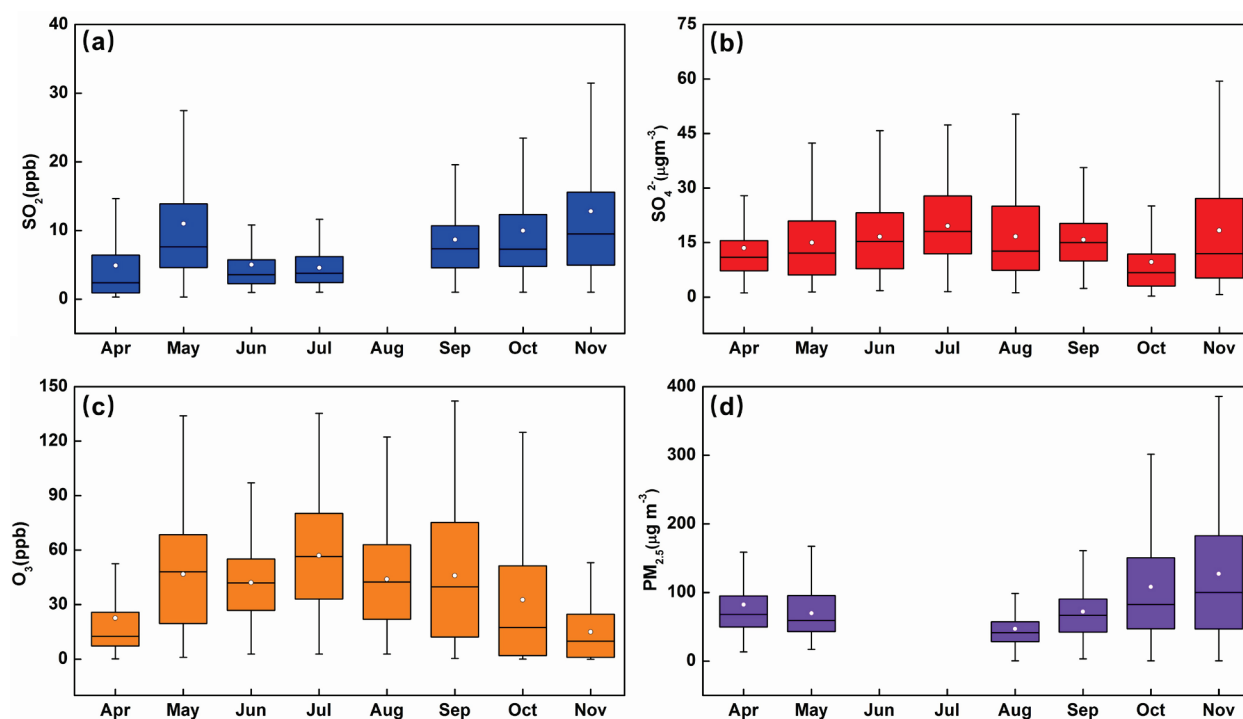

Fig. 3. Monthly average concentrations of (a) SO_2, (b) fine sulfate, (c) O_3, and (d) $PM_{2.5}$ in urban Ji'nan in 2015.
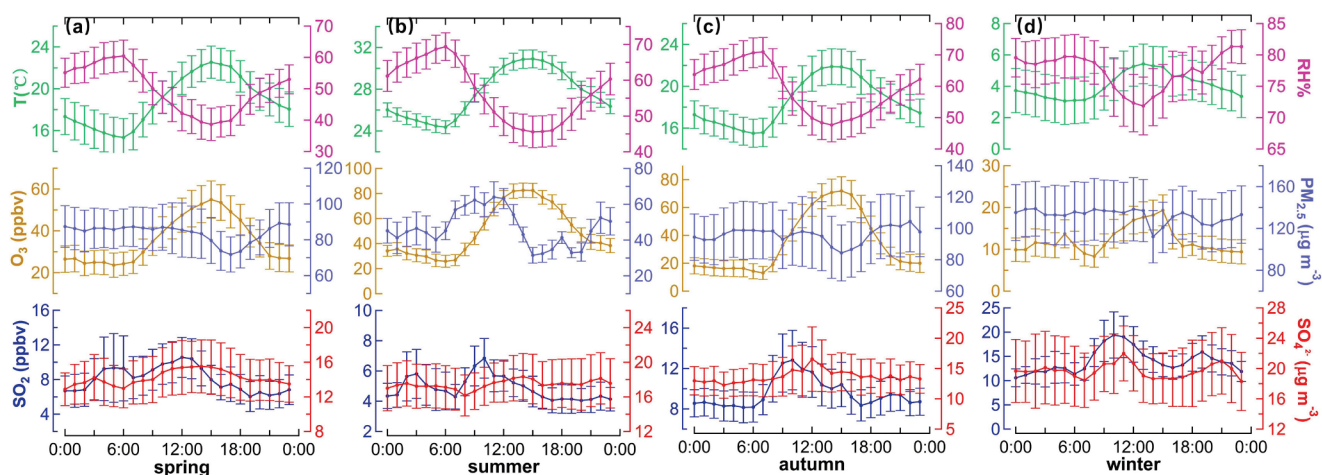
Fig. 4. Average diurnal variations in SO_2, fine sulfate, O_3, $PM_{2.5}$, temperature, and related humidity in (a) spring, (b) summer, (c) autumn, and (d) winter in urban Ji'nan in 2015. The error bars represent a quarter of the standard deviation.
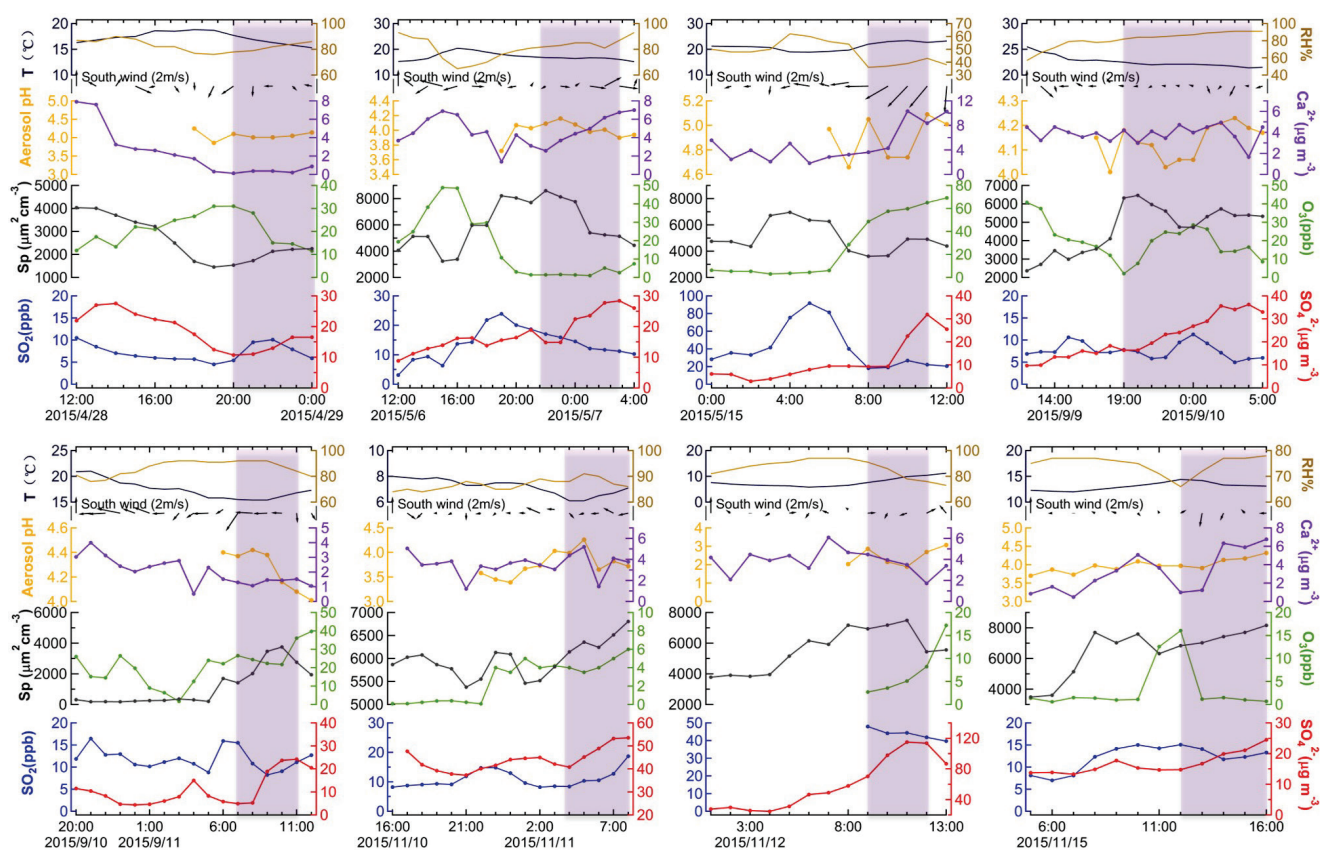

Fig. 5. Time series of the parameters of temperature, relative humidity, wind, aerosol pH, aerosol surface area density, and concentrations of calcium, O_3, SO_2, and fine sulfate in the eight selected cases (April 28, May 6 and 15, September 9 and 11, November 11, 12, and 15 in 2015 in urban Ji'nan). The shaded areas indicate the periods when significant sulfate production was observed.

mass. The shaded areas in Fig. 5 indicate the periods when significant sulfate production was observed. The secondary formation of sulfate happened near the sampling site or at the transport path from neighboring areas.

In the eight selected cases, the observed sulfate production rate was in the range of 1.1–10.8 µg m^{-3} h^{-1}. The fastest sulfate production rate appeared during the daytime of

November 12 and was accompanied by a high loading of $PM_{2.5}$ (313.0–519.4 µg m^{-3}) and high relative humidity (76%–91%). The second-fastest sulfate production rate (5.7 µg m^{-3} h^{-1}) occurred during the daytime on May 15 and was accompanied by a high concentration of ozone (48.7–65.1 ppbv). The aerosol pH was in the range of 1.6–5.1 in all eight cases, which is generally consistent with the

aerosol pH values in urban Beijing in North China (3.0–4.9) (Liu *et al.*, 2017) and in urban Guangzhou in South China (0.5–4.0) (Jia *et al.*, 2018). Ambient temperature and relative humidity ranged from 6.1 to 23.4°C and from 36% to 92%, respectively. In addition, the concentrations of OH radicals and H_2O_2 were estimated using the Master Chemical Mechanism model (MCM), which has been used in our previous studies to simulate RO_x chemistry (Xue *et al.*, 2016b). In all eight cases, the estimated concentration of OH radicals was in the range of 0.1×10^6–15×10^6 molecule cm^{-3}, which is comparable to the range observed at a rural site in North China during the summer (0×10^6–20×10^6 molecule cm^{-3}) (Tan *et al.*, 2017). The estimated H_2O_2 mixing ratio ranged from 0.1 to 2.5 ppbv, close to the values for other field measurements in this region (mostly 0.2–6.0 ppbv) (Wang *et al.*, 2016b). With the above data as inputs, the sulfate production rates via each pathway were calculated based on the methods described in Section 2.3. Note that the sum of the calculated contributions of the five pathways only accounted for 45.7%–73.8% of the observed sulfate production, the remaining fraction was mainly ascribed to other formation pathways such as SO_2 oxidation by Criegee intermediates in the gas-phase, by O_2 (catalyzed by transition metals), organic peroxides, and OH radicals in aqueous phase, and potential missing sources. Besides, significant uncertainty exists in the estimated aerosol pH and the adopted SO_2 uptake coefficient on the aerosol surface, which consequently lead to some inaccuracy to the calculated contributions.

As shown in Fig. 6, the gas-phase and aqueous-phase oxidation of SO_2 by photochemical oxidants contributed a large fraction to sulfate formation particularly during the daytime in warm season. Among the several photochemical oxidants, the contribution of gas-phase oxidation by OH radicals varied from 4.4%–51.2%, which is comparable to the sulfate formation in Hong Kong in South China during the daytime in winter (28%–32%) and in megacities in eastern China during heavy haze-fog events in cold season

(~3.1%) (Xue *et al.*, 2014, 2016a). The higher values occurred during daytime in warm seasons due to intensive solar radiation. During the daytime on May 15, the high mixing ratios of OH radicals (4.3×10^6–12×10^6 molecule cm^{-3}) greatly promoted the gas-phase oxidation of SO_2, and as a result, this pathway yielded a very high contribution of 51.2% to the total sulfate formation rate. Aqueous-phase oxidation by H_2O_2 made a minor contribution (0.3%–9.4%) to the sulfate formation during both daytime and nighttime in both warm and cold seasons, close to the values in Hong Kong during in South China the daytime in winter (5%–7%) and in megacities in eastern China during heavy haze-fog events in cold season (~0.9%) (Xue *et al.*, 2014, 2016a). During the daytime on November 12, the high aerosol acidity (1.6 < pH < 2.9) facilitated the sulfate formation via aqueous-phase SO_2 oxidation by H_2O_2, resulting in a contribution of 9.4%. During the daytime on May 15, there was little liquid water due to low humidity (36%–43%), and thus the aqueous-phase oxidation by H_2O_2 only contributed 0.3% to sulfate formation. As for the oxidants of O_3 and NO_2, the aqueous-phase oxidations contributed negligible fractions to sulfate production, owning to the acidic aerosol property of this region (as shown in Fig. 6), which was generally consistent with the calculation results in urban Beijing in North China (Guo *et al.*, 2017; Liu *et al.*, 2017).

The heterogeneous reactions of SO_2 on aerosol surfaces contributed a very large proportion to the total sulfate production rate at all times of day in cold seasons and at nighttime in warm seasons. During the daytime cases on November 12 and 15, the very high levels of aerosol surface area density (5438–7484 μm^2 cm^{-3} and 6835–8162 μm^2 cm^{-3}, respectively) promoted the sulfate formation via heterogeneous reaction of SO_2, which accounted for approximately 50.9% and 65.7%, respectively. In the four nighttime cases, the contribution of this formation pathway was in the range of 30.1%–62.7%. Furthermore, the five cases with large contribution (> 40%) of heterogeneous reactions all appeared when the aerosol surface area density
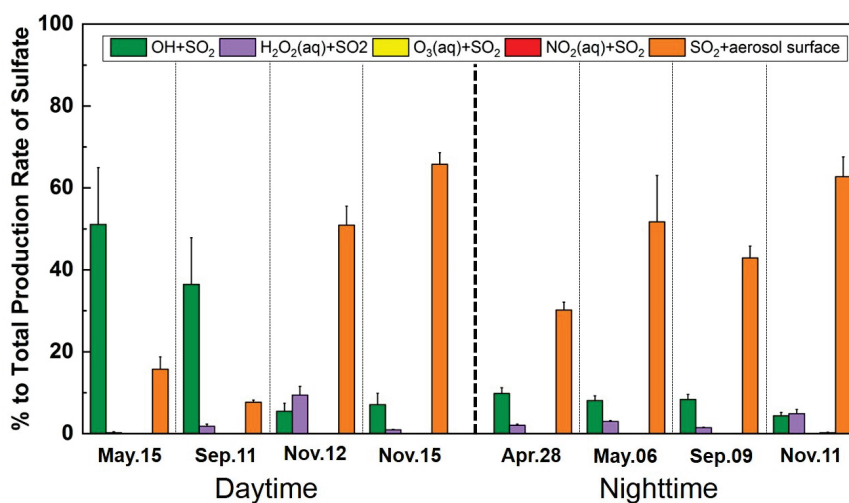

Fig. 6. Contributions of each of the five formation pathways to the total sulfate production rates in the eight selected cases (April 28, May 6 and 15, September 9 and 11, November 11, 12, and 15 in 2015 in urban Ji'nan). The error bars represent half of the standard deviation.

was high (> 5000 $\mu m^2\ cm^{-3}$) and the calcium concentration was high (most above 3.5 $\mu g\ m^{-3}$). The large contribution of the heterogeneous reactions of SO_2 on aerosol surfaces was primarily attributed to the very high aerosol loading and abundant dust particles in this region (Huang *et al.*, 2014b; Zhang *et al.*, 2015; Bai *et al.*, 2017) and also benefited from the relatively high humidity at nighttime.

To enhance the temporal representativeness of the calculation results on the contributions of different formation pathways to fine sulfate formation, additional eight cases in warm and cold seasons with fewer restrictions (maximum hourly sulfate concentration below 20 $\mu g\ m^{-3}$ in the cases on May 22 and November 27) were chosen and analyzed (see Figs. S2 and S3). The results are similar to those shown in Fig. 6, confirming the importance of SO_2 oxidation by photochemical oxidants at the daytime in warm season and the dominant role of heterogeneous reactions of SO_2 in cold season. Overall, the sulfate production in urban Ji'nan was dominated by SO_2 oxidation via photochemical oxidants during the day in warm seasons and by heterogeneous SO_2 reactions on aerosol surfaces at all times of day in cold seasons and at nighttime in warm seasons. Therefore, the aggravating photochemical pollution caused by the rising VOCs (Ma *et al.*, 2016; Sun *et al.*, 2016) and the increasing amount of dust particles caused by accelerated urbanization in the past decade are believed to be responsible for the rising sulfur oxidation ratio and thus the slow decrease in sulfate concentrations in urban Ji'nan. Therefore, strict control measures to control photochemical pollution and to reduce urban dust emissions are needed to efficiently mitigate the fine sulfate pollution in urban areas in North China.

SUMMARY AND CONCLUSIONS

To understand the trends in temporal variations in fine sulfate in North China and the factors that strongly influence the ambient concentration and secondary formation of fine sulfate, field measurements of fine sulfate and the related air pollutants and parameters were conducted in urban Ji'nan in 2015. Drawing on relevant data from previous studies of urban areas in Ji'nan, this study identified a significant decrease in the sulfate concentration over the period of 2008 till 2015, with an average decline rate of $-3.86 \pm 2.50\ \mu g\ m^{-3}\ yr^{-1}$ ($-10.0\ \%\ yr^{-1}$). The significant reduction in the sulfate concentration was facilitated by the implementation of a series of desulfurization techniques. However, the sulfate concentration decreased at a substantially slower rate than the SO_2 mixing ratios during the same period ($-11.6\ \%\ yr^{-1}$) due to a rising sulfur oxidation ratio. In 2015, the fine sulfate concentration in urban Ji'nan exhibited higher concentrations in summer and winter than spring and autumn, and in all seasons, the concentration was higher during the daytime than the nighttime due to the mixing ratios of SO_2 and oxidants, aerosol loading, and meteorological conditions. The observational data collected during the selected daytime and nighttime pollution cases showed that fine sulfate formed at rates of 1.1–10.8 $\mu g\ m^{-3}\ h^{-1}$. Among the various formation pathways, SO_2 oxidation by OH radicals and H_2O_2 dominated during the daytime in

warm seasons, whereas heterogeneous reactions of SO_2 were the dominant driver in cold seasons and at nighttime in warm seasons. Given the enhancement of photochemical oxidants and the increase in dust particles in recent years, the severe photochemical pollution and large emission of dust particles caused by rapid urbanization are likely responsible for the rising sulfur oxidation ratio and the slow reduction of sulfate concentrations and thus should be paid close attention in the future.

ACKNOWLEDGEMENTS

SUPPLEMENTARY MATERIAL

Supplementary data associated with this article can be found in the online version at http://www.aaqr.org.

REFERENCES

Anonymity (2017). Pollution characteristics of particulate matters and a dust storm episode in the spring of Tianjin. *Environmental Science & Technology of China*. Under review. (In Chinese with Abstract in English).

Bai, Z., Han, J. and Azzi, M. (2017). Insights into measurements of ambient air $PM_{2.5}$ in China. *TrAC, Trends Anal. Chem.* 13: 1–9.

Cao, J.J., Shen, Z.X., Chow, J.C., Watson, J.G., Lee, S.C., Tie, X.X., Ho, K.F., Wang, G.H. and Han, Y.M. (2012). Winter and summer $PM_{2.5}$ chemical compositions in fourteen Chinese cities. *J. Air Waste Manage. Assoc*. 62: 1214–1226.

Cheng, Y., Zheng, G., Wei, C., Mu, Q., Zheng, B., Wang, Z., Gao, M., Zhang, Q., He, K. and Carmichael, G. (2016). Reactive nitrogen chemistry in aerosol water as a source of sulfate during haze events in China. *Sci. Adv.* 2: e1601530.

Fairlie, T.D., Jacob, D.J., Dibb, J.E., Alexander, B., Avery, M.A., van Donkelaar, A. and Zhang, L. (2010). Impact of mineral dust on nitrate, sulfate, and ozone in transpacific Asian pollution plumes. *Atmos. Chem. Phys*. 10: 3999–4012.

Fang, C., Zhang, Z., Jin, M., Zou, P. and Wang, J. (2017). Pollution characteristics of $PM_{2.5}$ aerosol during haze periods in Changchun, China. *Aerosol Air Qual. Res.* 17: 888–895.

Fang, D., Wang, Q., Li, H., Yu, Y., Lu, Y. and Qian, X. (2016). Mortality effects assessment of ambient $PM_{2.5}$ pollution in the 74 leading cities of China. *Sci. Total Environ*. 569–570: 1545–1552.

Fountoukis, C. and Nenes, A. (2007). ISORROPIA II: A computationally efficient thermodynamic equilibrium model for K^+–Ca^{2+}–Mg^{2+}–NH_4^+–Na^+–SO_4^{2-}–NO_3^-–Cl^-–

H₂O Aerosols. *Atmos. Chem. Phys.* 7: 4639–4659.

Fu, X., Wang, S., Chang, X., Cai, S., Xing, J. and Hao, J. (2016). Modeling analysis of secondary inorganic aerosols over China: Pollution characteristics, and meteorological and dust impacts. *Sci. Rep.* 6: 35992.

Fu, X., Wang, S., Xing, J., Zhang, X., Wang, T. and Hao, J. (2017). Increasing ammonia concentrations reduce the effectiveness of particle pollution control achieved via SO₂ and NOₓ emissions reduction in east China. *Environ. Sci. Technol. Lett.* 4: 221–227.

Gao, X., Yang, L., Cheng, S., Gao, R., Zhou, Y., Xue, L., Shou, Y., Wang, J., Wang, X., Nie, W., Xu, P. and Wang, W. (2011). Semi-continuous measurement of water-soluble ions in PM₂.₅ in Jinan, China: Temporal variations and source apportionments. *Atmos. Environ.* 45: 6048–6056.

Gu, J., Du, S., Han, D., Hou, L., Yi, J., Xu, J., Liu, G., Han, B., Yang, G. and Bai, Z.P. (2014). Major chemical compositions, possible sources, and mass closure analysis of PM₂.₅ in Jinan, China. *Air Qual. Atmos. Health* 7: 251–262.

Guo, H., Weber, R.J. and Nenes, A. (2017). High levels of ammonia do not raise fine particle pH sufficiently to yield nitrogen oxide-dominated sulfate production. *Sci. Rep.* 7: 12109.

He, H., Wang, Y., Ma, Q., Ma, J., Chu, B., Ji, D., Tang, G., Liu, C., Zhang, H. and Hao, J. (2014). Mineral dust and NOₓ promote the conversion of SO₂ to sulfate in heavy pollution days. *Sci. Rep.* 4: 4172.

Huang, R.J., Zhang, Y., Bozzetti, C., Ho, K.F., Cao, J.J., Han, Y., Daellenbach, K.R., Slowik, J.G., Platt, S.M., Canonaco, F., Zotter, P., Wolf, R., Pieber, S.M., Bruns, E.A., Crippa, M., Ciarelli, G., Piazzalunga, A., Schwikowski, M., Abbaszade, G., Schnelle-Kreis, J., Zimmermann, R., An, Z., Szidat, S., Baltensperger, U., El Haddad, I. and Prevot, A.S. (2014a). High secondary aerosol contribution to particulate pollution during haze events in China. *Nature* 514: 218–222.

Huang, X., Song, Y., Zhao, C., Li, M., Zhu, T., Zhang, Q. and Zhang, X. (2014b). Pathways of sulfate enhancement by natural and anthropogenic mineral aerosols in China. *J. Geophys. Res.* 119: 14165–14179.

Huang, X., Liu, Z., Liu, J., Hu, B., Wen, T., Tang, G., Zhang, J., Wu, F., Ji, D., Wang, L. and Wang, Y. (2017). Chemical characterization and synergetic source apportionment of PM₂.₅ at multiple sites in the Beijing-Tianjin-Hebei region, China. *Atmos. Chem. Phys.* 17: 12941–12962.

Jia, S., Wang, X., Zhang, Q., Sarkar, S., Wu, L., Huang, M., Zhang, J. and Yang, L. (2018). Technical Note: Comparison and interconversion of pH based on different standard states for aerosol acidity characterization. *Atmos. Chem. Phys. Discuss.*, in Review.

Jiang, J., Zhou, W., Cheng, Z., Wang, S., He, K. and Hao, J. (2015). Particulate matter distributions in China during a winter period with frequent pollution episodes (January 2013). *Aerosol Air Qual. Res.* 15: 494–503.

Krotkov, N.A., McLinden, C.A., Li, C., Lamsal, L.N., Celarier, E.A., Marchenko, S.V., Swartz, W.H., Bucsela, E.J., Joiner, J. and Duncan, B.N. (2016). Aura omi observations of regional SO₂ and NO₂ pollution changes from 2005 to 2015. *Atmos. Chem. Phys.* 16: 4605–4629.

Li, B., Gasser, T., Ciais, P., Piao, S., Tao, S., Balkanski, Y., Hauglustaine, D., Boisier, J.P., Chen, Z., Huang, M., Li, L.Z., Li, Y., Liu, H., Liu, J., Peng, S., Shen, Z., Sun, Z., Wang, R., Wang, T., Yin, G., Yin, Y., Zeng, H., Zeng, Z. and Zhou, F. (2016). The contribution of China's emissions to global climate forcing. *Nature* 531: 357–361.

Li, G., Wang, Y. and Zhang, R. (2008). Implementation of a two-moment bulk microphysics scheme to the WRF model to investigate aerosol-cloud interaction. *J. Geophys. Res.* 113: D15211.

Li, H., Duan, F., Ma, Y., He, K., Zhu, L., Ma, T., Ye, S., Yang, S., Huang, T. and Kimoto, T. (2018). Haze pollution in winter and summer in Zibo, a heavily industrialized city neighboring the Jin-Jin-Ji area of China: Source, formation, and implications. *Atmos. Chem. Phys. Discuss.*, in Review.

Li, M., Zhang, Q., Kurokawa, J. I., Woo, J. H., He, K., Lu, Z., Ohara, T., Song, Y., Streets, D. G., Carmichael, G. R., Cheng, Y., Hong, C., Huo, H., Jiang, X., Kang, S., Liu, F., Su, H. and Zheng, B. (2017a). MIX: A mosaic Asian anthropogenic emission inventory under the international collaboration framework of the MICS-Asia and HTAP. *Atmos. Chem. Phys.* 17: 935–963.

Li, R., Yang, X., Fu, H., Hu, Q., Zhang, L. and Chen, J. (2017b). Characterization of typical metal particles during haze episodes in Shanghai, China. *Chemosphere* 181: 259–269.

Liu, F., Zhang, Q., Tong, D., Zheng, B., Li, M., Huo, H. and He, K.B. (2015a). High-resolution inventory of technologies, activities, and emissions of coal-fired power plants in China from 1990 to 2010. *Atmos. Chem. Phys.* 15: 13299–13317.

Liu, M., Song, Y., Zhou, T., Xu, Z., Yan, C., Zheng, M., Wu, Z., Hu, M., Wu, Y. and Zhu, T. (2017). Fine particle pH during severe haze episodes in Northern China. *Geophys. Res. Lett.* 44: 5213–5221.

Liu, X., Sun, K., Qu, Y., Hu, M., Sun, Y., Zhang, F. and Zhang, Y. (2015b). Secondary formation of sulfate and nitrate during a haze episode in megacity Beijing, China. *Aerosol Air Qual. Res.* 15: 2246–2257.

Ma, Z., Xu, J., Quan, W., Zhang, Z., Lin, W. and Xu, X. (2016). Significant increase of surface ozone at a rural site, north of Eastern China. *Atmos. Chem. Phys.* 16: 3969–3977.

Pope III, C.A., Burnett, R.T., Thun, M.J., Calle, E.E., Krewski, D., Ito, K. and Thurston, G.D. (2002). Lung cancer, cardiopulmonary mortality, and long-term exposure to fine particulate air pollution. *JAMA* 287: 1132–1141.

Sarwar, G., Fahey, K., Kwok, R., Gilliam, R.C., Roselle, S.J., Mathur, R., Xue, J., Yu, J. and Carter, W.P.L. (2013). Potential impacts of two SO₂ oxidation pathways on regional dulfate concentrations: Aqueous-phase oxidation by NO₂ and gas-phase oxidation by stabilized criegee intermediates. *Atmos. Environ.* 68: 186–197.

Seinfeld, J.H. and Pandis, S.N. (2006). *From air pollution*

to climate change, 2nd Edn, John Wiley & Sons Inc, New York.

Shen, X., Lee, T., Guo, J., Wang, X., Li, P., Xu, P., Wang, Y., Ren, Y., Wang, W., Wang, T., Li, Y., Carn, S.A. and Collett, J.L. (2012). Aqueous phase sulfate production in clouds in Eastern China. *Atmos. Environ.* 62: 502–511.

Sun, L., Xue, L., Wang, T., Gao, J., Ding, A., Cooper, O.R., Xu, P., Wang, Z., Wang, X., Wen, L., Zhu, Y., Chen, T., Yang, L., Wang, Y., Chen, J. and Wang, W. (2016). Significant increase of summertime ozone at Mt. Tai in Central Eastern China: 2003-2015. *Atmos. Chem. Phys.* 16: 10637–10650.

Tan, Z., Fuchs, H., Lu, K., Hofzumahaus, A., Bohn, B., Broch, S., Dong, H., Gomm, S., Häseler, R. and He, L. (2017). Radical chemistry at a rural site (Wangdu) in the North China Plain: Observation and model calculations of OH, HO$_2$ and RO$_2$ radicals. *Atmos. Chem. Phys.* 17: 663–690.

Wang, G., Zhang, R., Gomez, M.E., Yang, L., Zamora, M.L., Hu, M., Lin, Y., Peng, J., Guo, S. and Meng, J. (2016a). Persistent sulfate formation from London Fog to Chinese haze. *Proc. Natl. Acad. Sci. U.S.A.* 113: 13630–13635.

Wang, K., Zhang, Y., Nenes, A. and Fountoukis, C. (2012). Implementation of dust emission and chemistry into the community multiscale air quality modeling system and initial application to an Asian dust storm episode. *Atmos. Chem. Phys.* 12: 10209–10237.

Wang, L., Wen, L., Xu, C., Chen, J., Wang, X., Yang, L., Wang, W., Yang, X., Sui, X., Yao, L. and Zhang, Q. (2015). HONO and its potential source particulate nitrite at an urban site in North China during the cold season. *Sci. Total Environ.* 538: 93–101.

Wang, S., Xing, J., Zhao, B., Jang, C. and Hao, J. (2014a). Effectiveness of national air pollution control policies on the air quality in metropolitan areas of China. *J. Environ. Sci.* 26: 13–22.

Wang, X., Chen, J., Sun, J., Li, W., Yang, L., Wen, L., Wang, W., Wang, X., Collett, J.L., Jr., Shi, Y., Zhang, Q., Hu, J., Yao, L., Zhu, Y., Sui, X., Sun, X. and Mellouki, A. (2014b). Severe haze episodes and seriously polluted fog water in Ji'nan, China. *Sci. Total Environ.* 493: 133–137.

Wang, Y., Zhuang, G., Tang, A., Yuan, H., Sun, Y., Chen, S. and Zheng, A. (2005). The ion chemistry and the source of PM$_{2.5}$ aerosol in Beijing. *Atmos. Environ.* 39: 3771–3784.

Wang, Y., Wan, Q., Meng, W., Liao, F., Tan, H. and Zhang, R. (2011). Long-term impacts of aerosols on precipitation and lightning over the Pearl River Delta megacity area in China. *Atmos. Chem. Phys.* 11: 12421–12436.

Wang, Y., Chen, Z., Wu, Q., Liang, H., Huang, L., Li, H., Lu, K., Wu, Y., Dong, H., Zeng, L. and Zhang, Y. (2016b). Observation of atmospheric peroxides during Wangdu campaign 2014 at a rural site in the North China Plain. *Atmos. Chem. Phys.* 16: 10985–11000.

Xia, Y., Zhao, Y. and Nielsen, C.P. (2016). Benefits of China's efforts in gaseous pollutant control indicated by the bottom-up emissions and satellite observations 2000–2014. *Atmos. Environ.* 136: 43–53.

Xu, P., Wang, W., Yang, L., Zhang, Q., Gao, R., Wang, X., Nie, W. and Gao, X. (2011). Aerosol size distributions in urban Jinan: Seasonal characteristics and variations between weekdays and weekends in a heavily polluted atmosphere. *Environ. Monit. Assess.* 179: 443–456.

Xue, J., Yuan, Z., Yu, J.Z. and Ying, F. (2014). An observation-based model for secondary inorganic aerosols. *Aerosol Air Qual. Res.* 14: 862–878.

Xue, J., Yuan, Z., Griffith, S.M., Yu, X., Lau, A.K. and Yu, J.Z. (2016a). Sulfate formation enhanced by a cocktail of high NO$_x$, SO$_2$, particulate matter, and droplet pH during haze-fog events in megacities in China: An observation-based modeling investigation. *Environ. Sci. Technol.* 50: 7325–7334.

Xue, L., Gu, R., Wang, T., Wang, X., Saunders, S., Blake, D., Louie, P.K.K., Luk, C.W.Y., Simpson, I., Xu, Z., Wang, Z., Gao, Y., Lee, S., Mellouki, A. and Wang, W. (2016b). Oxidative capacity and radical chemistry in the polluted atmosphere of Hong Kong and Pearl River Delta Region: Analysis of a severe photochemical smog episode. *Atmos. Chem. Phys.* 16: 9891–9903.

Yang, L., Zhou, X., Wang, Z., Zhou, Y., Cheng, S., Xu, P., Gao, X., Nie, W., Wang, X. and Wang, W. (2012). Airborne fine particulate pollution in Jinan, China: concentrations, chemical compositions and influence on visibility impairment. *Atmos. Environ.* 55: 506–514.

Yue, D., Zhong, L., Zhang, T., Shen, J., Zhou, Y., Zeng, L., Dong, H. and Ye, S. (2015). Pollution properties of water-soluble secondary inorganic ions in atmospheric PM$_{2.5}$ in the Pearl River Delta Region. *Aerosol Air Qual. Res.* 15: 1737–1747.

Zhang, L., Liu, L., Zhao, Y., Gong, S., Zhang, X., Henze, D.K., Capps, S.L., Fu, T.M., Zhang, Q. and Wang, Y. (2015). Source attribution of particulate matter pollution over North China with the adjoint method. *Environ. Res. Lett.* 10: 084011.

Zhao, X., Zhao, P., Xu, J., Meng, W., Pu, W., Dong, F., He, D. and Shi, Q. (2013). Analysis of a winter regional haze event and its formation mechanism in the North China Plain. *Atmos. Chem. Phys.* 13: 5685–5696.

Zhao, Y., Duan, L., Xing, J., Larssen, T., Nielsen, C.P. and Hao, J. (2009). Soil acidification in China: Is controlling SO$_2$ emissions enough?. *Environ. Sci. Technol.* 43: 8021–8026.

Zheng, B., Zhang, Q., Zhang, Y., He, K.B., Wang, K., Zheng, G.J., Duan, F.K., Ma, Y.L. and Kimoto, T. (2015). Heterogeneous chemistry: A mechanism missing in current models to explain secondary inorganic aerosol formation during the January 2013 haze episode in North China. *Atmos. Chem. Phys.* 15: 2031–2049.